Frontiers of Information Technology & Electronic Engineering
www.jzus.zju.edu.cn; engineering.cae.cn; www.springerlink.com
ISSN 2095-9184 (print); ISSN 2095-9230 (online)
E-mail: jzus@zju.edu.cn

An optimized formula for the two-point resistance of a cobweb resistance network and its potential application*

Yu GUAN[1], Xiaoyu JIANG†‡[1], Yanpeng ZHENG†‡[2], Zhaolin JIANG[3]

[1]*School of Information Science and Engineering, Linyi University, Linyi 276000, China*

[2]*School of Automation and Electrical Engineering, Linyi University, Linyi 276000, China*

[3]*School of Mathematics and Statistics, Linyi University, Linyi 276000, China*

†E-mail: jxy19890422@sina.com; zhengyanpeng0702@sina.com

Received July 21, 2024; Revision accepted Oct. 10, 2024; Crosschecked May 6, 2025

Abstract: In recent years, the exploration and application of resistance networks have expanded significantly, and solving the equivalent resistance between two points of a resistance network has been an important topic. In this paper, we focus on optimizing the formula for calculating the two-point resistance of an $m \times n$ cobweb resistance network with $2r$ boundary conditions. To improve the computational efficiency of the equivalent resistance between two points, the formula is optimized by using the optimal approximation property of Chebyshev polynomials in combination with hyperbolic functions, and the derivation process is simplified. We discuss the equivalent resistance formulas in several special cases and compare the computational efficiency of the equivalent resistance formulas before and after optimization. Finally, we make an innovative attempt at path planning through potential formulas and propose a heuristic algorithm based on cobweb potential function for robot path planning in a cobweb environment with obstacles.

Key words: Resistance network; Equivalent resistance; Potential function; Chebyshev polynomials; Path planning
https://doi.org/10.1631/FITEE.2400613 **CLC number:** TM13; O441.1

1 Introduction

With the continuous progress of modern science, many fields are facing increasingly complex problems. Further exploration by the researchers found that building a resistance network model (Kirchhoff, 1847; Pennetta et al., 2004; Ferri and Antonini, 2007; Owaidat et al., 2012; Rhazaoui et al., 2013; Liu et al., 2016; Hadad et al., 2018; Xu et al., 2021; Zhang et al., 2021) can help solve some of these problems. Since Kirchhoff's law (Kirchhoff, 1847) laid the foundation for the research of resistance networks, after more than 170 years of in-depth exploration, the research of resistance networks has made remarkable progress and researchers have proposed some new methods.

In the early days, the research of resistance networks focused on infinite network structures, and Cserti et al. (2002) opened a completely new path for the exploration of infinite resistance networks by introducing Green's function technique. Subsequently, the equivalent resistance values between any two points in various infinite lattice resistance structures were accurately computed using this method (Cserti et al., 2011), and the method was extended to deal with perturbed lattice problems containing one missing bond (Giordano, 2007). Since then, Green's function techniques have been gradually applied to the research of infinite networks, and some new theoretical results have been obtained (Giordano, 2007; Hijjawi et al., 2008; Guttmann, 2010; Kook, 2011;

‡ Corresponding authors

* Project supported by the National Natural Science Foundation of China (No. 12101284), the Natural Science Foundation of Shandong Province (No. ZR2022MA092), and the Department of Education of Shandong Province (No. 2023KJ214)

ORCID: Xiaoyu JIANG, https://orcid.org/0000-0001-5857-9148; Yanpeng ZHENG, https://orcid.org/0000-0002-6874-9187

Asad, 2013a, 2013b; Asad et al., 2013). However, an infinite network is an ideal structure without considering boundary conditions, and Green's function techniques are not applicable to finite networks. The initial exploration of finite networks can be traced back to the research of Klein and Randić (1993), which was subsequently explored in more depth by Klein (2010) and Yang and Klein (2013). Meanwhile, Wu FY (2004) proposed a Laplacian matrix method to calculate the resistance between arbitrary nodes in a finite resistance lattice, which has been widely used in subsequent studies (Tzeng and Wu, 2006; Essam et al., 2014, 2015; Izmailian and Kenna, 2014, 2015; Izmailian et al., 2014). Specifically, Essam and Wu (2009) used the method to successfully find the exact value of the site-to-site resistance and its asymptotic expansion under free boundary conditions, while Izmailian and Huang (2010) further extended it to compute the resistance values under many different boundary conditions. However, the resistance between arbitrary nodes with complex boundary conditions cannot be solved using the Laplacian method.

To overcome the shortcomings of previous theories, Tan et al. (2013) creatively introduced the recursive transformation (RT) method, which opened up a new path for the study of resistance networks. Compared with the traditional Laplacian method that relies on two direction matrices, this method requires only one direction matrix. This not only simplifies the solving process but also makes the solution more convenient. For instance, it can be used to solve the equivalent resistance between two points in a cobweb with complex boundary conditions (Tan and Fang, 2015). Subsequently, Tan utilized the RT method to explore the electrical characteristics of resistance networks and made significant contributions to the development of the field (Tan, 2017, 2022, 2023a, 2023b; Tan ZZ and Tan Z, 2020a, 2020b, 2020c; Luo and Tan, 2023; Chen et al., 2024). The core of the RT method is to construct a recursive matrix equation containing a tridiagonal matrix. Nowadays, tridiagonal matrices have been widely studied (Jiang ZL et al., 2019; Wei et al., 2019a, 2019b, 2020, 2022; Fu et al., 2020a, 2020b; Meng QY et al., 2021, 2022a, 2022b; Wang JJ et al., 2023). In addition, neural networks (Wang XZ et al., 2017; Jin et al., 2022a, 2022b; Shi et al., 2022; Sun et al., 2022; Hu and Zheng, 2023; Wu WQ and Zhang, 2024) have similarities to resistance networks.

It is worth mentioning that Tan and Fang (2015) ingeniously established a mathematical model of a cobweb resistance network with $2r$ boundary resistance, which theoretically gives an incomparable accurate formula for the equivalent resistance between any two points. However, as the scale of the cobweb resistance network increases, the original resistance formula gradually reveals deficiencies in terms of computational performance and scalability. To compensate for these deficiencies, in this paper, Chebyshev polynomials of the second kind (Udrea, 1996; Mason and Handscomb, 2002) combined with hyperbolic functions are used to re-express the exact formula for the equivalent resistance between any two points, which significantly improves the computational efficiency. In recent years, some progress has been made in large-scale potential calculation (Zhou et al., 2022, 2023; Jiang ZL et al., 2023; Zhao et al., 2023; Jiang XY et al., 2024; Meng X et al., 2024; Wang R et al., 2024), which also provides ideas for this research.

Different from the existing research results, this paper focuses on a new resistance network model, the cobweb, which is re-represented by using Chebyshev polynomials of the second kind combined with hyperbolic functions on the basis of the original equivalent resistance formula between two points, giving the rederived equivalent resistance formula and the related proofs. By optimizing the original resistance formula, not only the derivation process is simplified but also the optimal approximation property of Chebyshev polynomials is skillfully incorporated, which significantly improves the computational efficiency and practicality of the optimized formula. Considering the influence of parameters on the equivalent resistance formula, the equivalent resistance formulas in several special cases are discussed in this paper and demonstrated in three-dimensional (3D) graphs. Comparative experiments on the equivalent resistance formulas before and after optimization reveal that the optimization greatly reduces the time cost. The equivalent resistance formula proposed in this paper is very suitable for the application to large-scale complex networks due to its high computational efficiency.

In addition, path planning methods have been extensively studied and applied in various fields, including collaborative mobile robots using discrete

event models (Mahulea et al., 2020), improved artificial potential fields for multiple unmanned aerial vehicles (multi-UAV) path optimization and control (Pan et al., 2022), hybrid methods combining water flow potential fields with beetle antennae search for mobile robot path planning (Yu et al., 2023), automatic ship collision avoidance (Zhu et al., 2023), and 3D potential field models for local path planning of autonomous vehicles (Ji et al., 2023). In recent years, as in-depth research on path planning problems with specific shapes has been conducted by researchers, a series of important achievements have emerged. Uğur (2008) and Xue et al. (2021) achieved breakthroughs in path planning research on cuboids and cylinders, respectively, while Kulathunga (2022) and Mazaheri et al. (2024) made a significant progress in path planning in 3D environments. These studies fully demonstrate the examples of path planning in special environments. In this context, based on the potential function of the cobweb resistance network, a path planning algorithm for robots in a cobweb environment is proposed. The algorithm optimizes the characteristics of the resistance network, computes the motion path of robots in the cobweb environment by a precise potential function, and realizes efficient and accurate path planning.

Tan and Fang (2015) proposed an $m\times n$ cobweb resistance network with $2r$ boundaries, which has n radial lines and m polygons (or circles). Bonds in the radial and arc directions represent resistors r_0 and r, respectively, except for a $2r$ boundary, and let O be the origin of the coordinate system in Fig. 1. Point $O(0,0)=0$ is defined as the origin of the resistance network. Assume that the input and output points of current J are represented by d_1 and d_2, respectively. The equivalent resistance between any two points $d_1(0,y_1)$ and $d_2(x,y_2)$ is as follows:

$$R_{m\times n}(\{0,y_1\},\{x,y_2\}) =\frac{2r}{m}\sum_{i=1}^{m}\frac{F_n^{(i)}(S_{1,i}^2+S_{1,i}^2)-2(F_x^{(i)}+F_{n-x}^{(i)})S_{1,i}S_{2,i}}{\lambda_i^n+\overline{\lambda}_i^n-2}, \tag{1}$$

where

$$F_k^{(i)}=(\lambda_i^k-\overline{\lambda}_i^k)/(\lambda_i-\overline{\lambda}_i),\ k=0,\ 1,\ \ldots,\ n, \tag{2}$$

$$h=r/r_0,\ \lambda_k\overline{\lambda}_k=1,\ k=1,\ 2,\ \ldots,\ m, \tag{3}$$

$$S_{k,i}=\sin(y_k\theta_i),\ \theta_i=(2i-1)\pi/(2m),\ i=1,\ 2,\ \ldots,\ m, \tag{4}$$

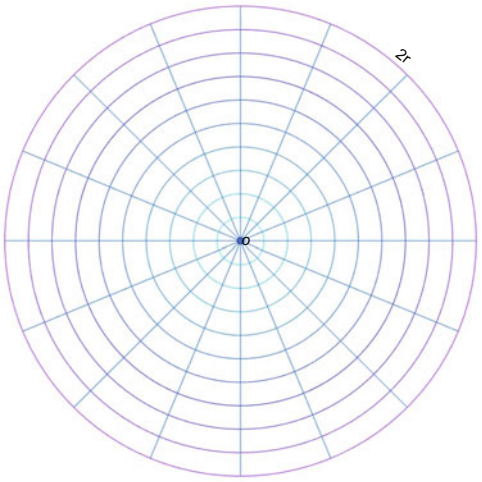

Fig. 1 A 10×16 cobweb with a $2r$ boundary, containing 10×16 nodes and a zero potential point O

$$\lambda_i=1+h-h\cos\theta_i+\sqrt{(1+h-h\cos\theta_i)^2-1}, \tag{5}$$

$$\overline{\lambda}_i=1+h-h\cos\theta_i-\sqrt{(1+h-h\cos\theta_i)^2-1}. \tag{6}$$

2 Optimized formula of resistance represented by Chebyshev polynomials

In this section, the resistance formula (1) for re-representing the cobweb resistance network is introduced. The equivalent resistance expression represented by Chebyshev polynomials of the second kind can improve the computational efficiency.

Let us consider a scenario where a current J flows in at $d_1(0,y_1)$ with $0\le y_1\le m$ and flows out at $d_2(x,y_2)$ with $0\le x\le n$ and $0\le y_2\le m$. The new resistance formula for the resistance of the $m\times n$ cobweb resistance network with a $2r$ boundary condition can be expressed as follows:

$$R_{m\times n}\{(0,y_1),(x,y_2)\} =\frac{2r}{m}\sum_{j=1}^{m}\frac{U_{n-1}^{(j)}(S_{1,j}^2+S_{2,j}^2)-2(U_{x-1}^{(j)}+U_{n-x-1}^{(j)})S_{1,j}S_{2,j}}{U_n^{(j)}-U_{n-2}^{(j)}-2}, \tag{7}$$

where

$$U_k^{(j)}=U_k^{(j)}(\cosh\psi_j)=\frac{\sinh(k+1)\psi_j}{\sinh\psi_j},$$

$$\cosh\psi_j=\frac{\kappa_j}{2},\ \frac{\kappa_j}{2}>1,\ \psi_j>0,\ k=0,\ 1,\ \ldots,\ n, \tag{8}$$

$$\kappa_j=2+2\frac{r}{r_0}-2\frac{r}{r_0}\cos\frac{(2j-1)\pi}{2m}, \tag{9}$$

$$S_{k,j}=\sin\frac{y_k(2j-1)\pi}{2m},\ k=1,\ 2. \tag{10}$$

3 Optimization process of the original function

In this section, to improve the actual performance, we introduce the Horadam sequence represented by Chebyshev polynomials of the second kind (Udrea, 1996; Mason and Handscomb, 2002).

The Horadam sequence is defined by the following conditions (Udrea, 1996):

$$W_k=dW_{k-1}-qW_{k-2},\ W_0=A,\ W_1=B, \tag{11}$$

where $k\in\mathbf{N},\ \ k\geq 2,\ \ A,\ B,\ d,\ q\in\mathbf{C}$, $\mathbf{N}$ is the set of all natural numbers, and $\mathbf{C}$ is the set of all complex numbers.

The Horadam sequence represented by Chebyshev polynomials of the second kind (Mason and Handscomb, 2002) is as follows:

$$W_k=(\sqrt{q})^k\left(\frac{B}{\sqrt{q}}U_{k-1}\left(\frac{d}{2\sqrt{q}}\right)-AU_{k-2}\left(\frac{d}{2\sqrt{q}}\right)\right), \tag{12}$$

where $q>0$, $k\geq 0$, and the Chebyshev polynomials of the second kind are defined as follows:

$$\begin{aligned}U_k=U_k(\cos\psi)&=\frac{\sin(k+1)\psi}{\sin\psi},\\ \cos\psi&=\frac{d}{2\sqrt{q}},\ \psi\in\mathbf{C},\ k\geq 0.\end{aligned} \tag{13}$$

If $\frac{d}{2\sqrt{q}}>1$, Chebyshev polynomials of the second kind are re-described by hyperbolic functions. Then, Eq. (13) should be expressed as follows:

$$\begin{aligned}U_k=U_k(\cosh\psi)&=\frac{\sinh(k+1)\psi}{\sinh\psi},\\ \cosh\psi&=\frac{d}{2\sqrt{q}},\ \psi\in\mathbf{R},\ k\geq 0,\end{aligned} \tag{14}$$

where $\mathbf{R}$ is the set of real numbers.

First, the derivation of Eq. (2) represented by Chebyshev polynomials of the second kind is given.

Remark 1 It can be obtained from Eqs. (5) and (6) that $\lambda_j+\overline{\lambda}_j=\kappa_j$ and $\lambda_j\overline{\lambda}_j=1$. By adding these conditions with Eq. (11), we obtain the following special Horadam sequence:

$$F_k^{(j)}=\kappa_jF_{k-1}^{(j)}-F_{k-2}^{(j)},\ F_0^{(j)}=0,\ F_1^{(j)}=1, \tag{15}$$

where $d=\kappa_j>2$, $q=1$, and $F_k^{(j)}$ and κ_j are given by Eqs. (2) and (9), respectively. By using Eqs. (2), (11), (12), and (14), the expression of $F_k^{(j)}$ can be obtained as follows:

$$F_k^{(j)}=\frac{\lambda_j^k-\overline{\lambda}_j^k}{\lambda_j-\overline{\lambda}_j}=U_{k-1}^{(j)}\left(\frac{\kappa_j}{2}\right),\ k=0,\ 1,\ \ldots,\ n. \tag{16}$$

Second, we give the derivation of $\lambda_j^n+\overline{\lambda}_j^n$ expressed by Chebyshev polynomials of the second kind.

Remark 2 Let

$$B_n^{(j)}=\lambda_j^n+\overline{\lambda}_j^n, \tag{17}$$

where $B_0^{(j)}=2$, $B_1^{(j)}=\kappa_j$.

Then, the recursive relation of $B_n^{(j)}$ is expressed as follows:

$$B_n^{(j)}=\kappa_jB_{n-1}^{(j)}-B_{n-2}^{(j)},\ B_0^{(j)}=2,\ B_1^{(j)}=\kappa_j, \tag{18}$$

where $d=\kappa_j$, $q=1$, and κ_j and $B_n^{(j)}$ are expressed in Eqs. (9) and (17), respectively.

By using Eqs. (12) and (14), $B_n^{(j)}$ is represented as follows:

$$\begin{aligned}B_n^{(j)}=\lambda_j^{(n)}+\overline{\lambda}_j^{(n)}&=\kappa_jU_{n-1}\left(\frac{\kappa_j}{2}\right)-2U_{n-2}\left(\frac{\kappa_j}{2}\right)\\ &=U_n\left(\frac{\kappa_j}{2}\right)-U_{n-2}\left(\frac{\kappa_j}{2}\right).\end{aligned} \tag{19}$$

Using Eqs. (14), (16), and (19), the equivalent resistance formula (7) is obtained.

4 Several interesting classes of the resistance network

This section is based on the obtained equivalent resistance formula (7) for a cobweb resistance network with multiple variables. We analyze the influence of different variables on the equivalent resistance expression, assign the corresponding variables according to the conditions, and draw a 3D view for visual display.

Special 1 When the current J flows from input point $d_1(0,y_1)$ to output point $d_2(x,y_2)$, where $y_1=y_2$ and $S_{1,j}=S_{2,j}$, the formula for the equivalent resistance between two points is as follows:

$$\begin{aligned}&R_{m\times n}(\{0,y_2\},\{x,y_2\})\\ =&\frac{4r}{m}\sum_{j=1}^{m}\frac{U_{n-1}^{(j)}-(U_{x-1}^{(j)}+U_{n-x-1}^{(j)})}{U_n^{(j)}-U_{n-2}^{(j)}-2}S_{k,j}^2,\ k=1,2,\end{aligned} \tag{20}$$

where

$$U_k^{(j)} = U_k^{(j)}(\cosh\psi_j) = \frac{\sinh(k+1)\psi_j}{\sinh\psi_j},$$
$$\cosh\psi_j = \frac{\kappa_j}{2},\ \frac{\kappa_j}{2} > 1,\ \psi_j > 0,\ k = 0,\ 1,\ \ldots,\ n, \tag{21}$$

$$\kappa_j = 2 + 2\frac{r}{r_0} - 2\frac{r}{r_0}\cos\frac{(2j-1)\pi}{2m}, \tag{22}$$

$$S_{k,j} = \sin\frac{y_k(2j-1)\pi}{2m},\ k = 1,\ 2. \tag{23}$$

Let $m = n = 60$ and $r_0 = r = 1$ in Eq. (20). We can obtain a special resistance formula for the cobweb resistance network as follows:

$$R_{60\times60}(\{0, y_2\}, \{x, y_2\}) = \frac{1}{15}\sum_{j=1}^{60}\frac{U_{59}^{(j)} - (U_{x-1}^{(j)} + U_{59-x}^{(j)})}{U_{60}^{(j)} - U_{58}^{(j)} - 2}S_{2,j}^2, \tag{24}$$

where

$$U_k^{(j)} = U_k^{(j)}(\cosh\psi_j) = \frac{\sinh(k+1)\psi_j}{\sinh\psi_j},$$
$$\cosh\psi_j = \frac{\kappa_j}{2},\ k = 0,\ 1,\ \ldots,\ n, \tag{25}$$

$$\kappa_j = 4 - 2\cos\frac{(2j-1)\pi}{120}, \tag{26}$$

$$S_{2,j} = \sin\frac{y_2(2j-1)\pi}{120}. \tag{27}$$

The 3D distribution of the equivalent resistance is shown in Fig. 2.

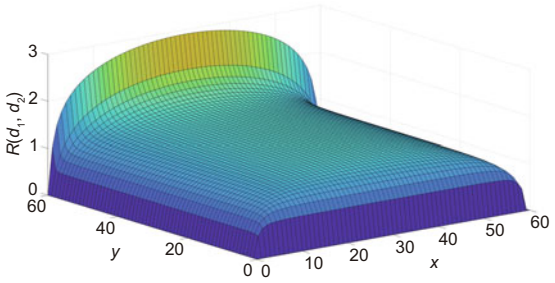

Fig. 2 The equivalent resistance view of $R_{60\times60}(d_1, d_2)$ with a cobweb resistance network shown in Eq. (24)

Special 2 If the current J flows in at point $d_1(0,0) = O(0,0)$ and flows out at $d_2(x, y_2)$, then the formula for the equivalent resistance between two points is as follows:

$$R_{m\times n}\{(0,0),(x,y_2)\} = \frac{2r}{m}\sum_{j=1}^{m}\frac{U_{n-1}^{(j)}S_{2,j}^2}{U_n^{(j)} - U_{n-2}^{(j)} - 2}, \tag{28}$$

where $U_k^{(j)}$ is defined in Eq. (21), κ_j is defined in Eq. (22), and $S_{k,j}$ is defined in Eq. (23).

Let $m = n = 60$ and $r_0 = r = 1$ in Eq. (28). We can obtain a special resistance formula for the cobweb resistance network as follows:

$$R_{60\times60}\{(0,0),(x,y_2)\} = \frac{1}{30}\sum_{j=1}^{60}\frac{U_{59}^{(j)}S_{2,j}^2}{U_{60}^{(j)} - U_{58}^{(j)} - 2}, \tag{29}$$

where

$$U_k^{(j)} = U_k^{(j)}(\cosh\psi_j) = \frac{\sinh(k+1)\psi_j}{\sinh\psi_j},$$
$$\cosh\psi_j = \frac{\kappa_j}{2},\ k = 0,\ 1,\ \ldots,\ n, \tag{30}$$

$$\kappa_j = 4 - 2\cos\frac{(2j-1)\pi}{120}, \tag{31}$$

$$S_{2,j} = \sin\frac{y_2(2j-1)\pi}{120}. \tag{32}$$

The 3D distribution of the equivalent resistance is shown in Fig. 3.

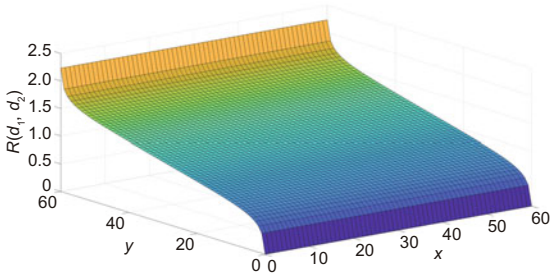

Fig. 3 The equivalent resistance view of $R_{60\times60}(d_1, d_2)$ with a cobweb resistance network shown in Eq. (29)

Special 3 If the current J flows in at point $d_1(0, y_1)$ and flows out at $d_2(20, y_2)$, then the formula for the equivalent resistance between two points is as follows:

$$R_{m\times n}\{(0,y_1),(20,y_2)\} = \frac{2r}{m}\sum_{j=1}^{m}\frac{U_{n-1}^{(j)}(S_{1,j}^2+S_{2,j}^2) - 2(U_{x-1}^{(j)}+U_{n-x-1}^{(j)})S_{1,j}S_{2,j}}{U_n^{(j)} - U_{n-2}^{(j)} - 2}, \tag{33}$$

where $U_k^{(j)}$ is defined in Eq. (21), κ_j is defined in Eq. (22), and $S_{k,j}$ is defined in Eq. (23).

Let $m = n = 60$ and $r_0 = r = 1$ in Eq. (33). We can obtain a special resistance formula for the

cobweb resistance network as follows:

$$R_{60\times60}\{(0,y_1),(20,y_2)\} =\frac{1}{30}\sum_{j=1}^{60}\frac{U_{59}^{(j)}(S_{1,j}^2+S_{2,j}^2)-2(U_{19}^{(j)}+U_{39}^{(j)})S_{1,j}S_{2,j}}{U_{60}^{(j)}-U_{58}^{(j)}-2}, \tag{34}$$

where

$$U_k^{(j)}=U_k^{(j)}(\cosh\psi_j)=\frac{\sinh(k+1)\psi_j}{\sinh\psi_j}, \quad \cosh\psi_j=\frac{\kappa_j}{2},\ k=0,\ 1,\ \ldots,\ n, \tag{35}$$

$$\kappa_j=4-2\cos\frac{(2j-1)\pi}{120}, \tag{36}$$

$$S_{1,j}=\sin\frac{y_1(2j-1)\pi}{120},\quad S_{2,j}=\sin\frac{y_2(2j-1)\pi}{120}. \tag{37}$$

The 3D distribution of the equivalent resistance is shown in Fig. 4.

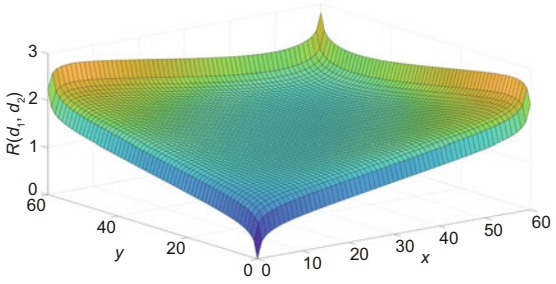

Fig. 4 The equivalent resistance view of $R_{60\times60}(d_1,d_2)$ with a cobweb resistance network shown in Eq. (34)

Special 4 When the current J flows from input point $d_1(0,y_1)$ to output point $d_2(x,y_2)$, where $y_1=x$, the formula for the equivalent resistance between two points is as follows:

$$R_{m\times n}\{(0,x),(x,y_2)\} =\frac{2r}{m}\sum_{j=1}^{m}\frac{U_{n-1}^{(j)}(S_{1,j}^2+S_{2,j}^2)-2(U_{x-1}^{(j)}+U_{n-x-1}^{(j)})S_{1,j}S_{2,j}}{U_n^{(j)}-U_{n-2}^{(j)}-2}, \tag{38}$$

where $U_k^{(j)}$ is defined in Eq. (21), κ_j is defined in Eq. (22), and $S_{k,j}$ is defined in Eq. (23).

Let $m=n=60$ and $r_0=r=1$ in Eq. (38). We can obtain a special resistance formula for the cobweb resistance network as follows:

$$R_{60\times60}\{(0,x),(x,y_2)\} =\frac{1}{30}\sum_{j=1}^{60}\frac{U_{59}^{(j)}(S_{1,j}^2+S_{2,j}^2)-2(U_{x-1}^{(j)}+U_{59-x}^{(j)})S_{1,j}S_{2,j}}{U_{60}^{(j)}-U_{58}^{(j)}-2}, \tag{39}$$

where

$$U_k^{(j)}=U_k^{(j)}(\cosh\psi_j)=\frac{\sinh(k+1)\psi_j}{\sinh\psi_j}, \quad \cosh\psi_j=\frac{\kappa_j}{2},\ k=0,\ 1,\ \ldots,\ n, \tag{40}$$

$$\kappa_j=4-2\cos\frac{(2j-1)\pi}{120}, \tag{41}$$

$$S_{1,j}=\sin\frac{x(2j-1)\pi}{120},\quad S_{2,j}=\sin\frac{y_2(2j-1)\pi}{120}. \tag{42}$$

The 3D distribution of the equivalent resistance is shown in Fig. 5.

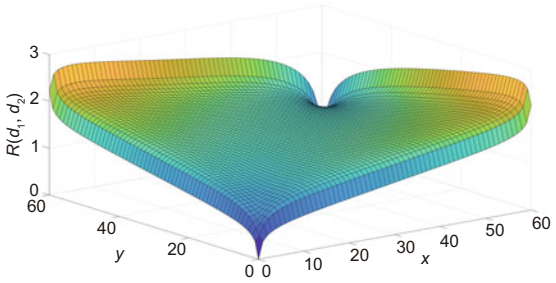

Fig. 5 The equivalent resistance view of $R_{60\times60}(d_1,d_2)$ with a cobweb resistance network shown in Eq. (39)

Special 5 When the current J flows from input point $d_1(0,y_1)$ to output point $d_2(x,y_2)$, where $y_2=x$, the formula for the equivalent resistance between two points is as follows:

$$R_{m\times n}\{(0,y_1),(x,x)\} =\frac{2r}{m}\sum_{j=1}^{m}\frac{U_{n-1}^{(j)}(S_{1,j}^2+S_{2,j}^2)-2(U_{x-1}^{(j)}+U_{n-x-1}^{(j)})S_{1,j}S_{2,j}}{U_n^{(j)}-U_{n-2}^{(j)}-2}, \tag{43}$$

where $U_k^{(j)}$ is defined in Eq. (21), κ_j is defined in Eq. (22), and $S_{k,j}$ is defined in Eq. (23).

Let $m=n=60$ and $r_0=r=1$ in Eq. (43). We can obtain a special resistance formula for the cobweb resistance network as follows:

$$R_{60\times60}\{(0,y_1),(x,x)\} =\frac{1}{30}\sum_{j=1}^{60}\frac{U_{59}^{(j)}(S_{1,j}^2+S_{2,j}^2)-2(U_{x-1}^{(j)}+U_{59-x}^{(j)})S_{1,j}S_{2,j}}{U_{60}^{(j)}-U_{58}^{(j)}-2}, \tag{44}$$

where

$$U_k^{(j)}=U_k^{(j)}(\cosh\psi_j)=\frac{\sinh(k+1)\psi_j}{\sinh\psi_j}, \quad \cosh\psi_j=\frac{\kappa_j}{2},\ k=0,\ 1,\ \ldots,\ n, \tag{45}$$

$$\kappa_j = 4 - 2\cos\frac{(2j-1)\pi}{120}, \tag{46}$$

$$S_{1,j} = \sin\frac{y_1(2j-1)\pi}{120}, \quad S_{2,j} = \sin\frac{x(2j-1)\pi}{120}. \tag{47}$$

The 3D distribution of the equivalent resistance is shown in Fig. 6.

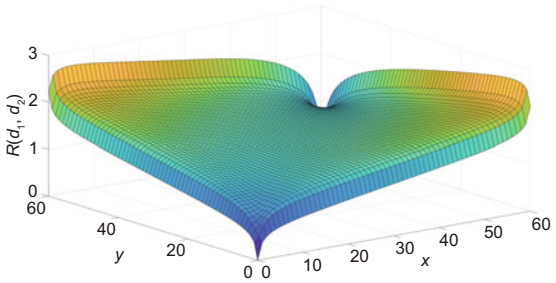

Fig. 6 The equivalent resistance view of $R_{60\times60}(d_1, d_2)$ with a cobweb resistance network shown in Eq. (44)

Special 6 If the current J flows in at point $d_1(0, y_1)$ and flows out at $d_2(x, 20)$, then the formula for the equivalent resistance between two points is as follows:

$$R_{m\times n}\{(0,y_1),(x,20)\} = \frac{2r}{m}\sum_{j=1}^{m}\frac{U_{n-1}^{(j)}(S_{1,j}^2+S_{2,j}^2)-2(U_{x-1}^{(j)}+U_{n-x-1}^{(j)})S_{1,j}S_{2,j}}{U_n^{(j)}-U_{n-2}^{(j)}-2}, \tag{48}$$

where $U_k^{(j)}$ is defined in Eq. (21), κ_j is defined in Eq. (22), and $S_{k,j}$ is defined in Eq. (23).

Let $m = n = 60$ and $r_0 = r = 1$ in Eq. (48). We can obtain a special resistance formula for the cobweb resistance network as follows:

$$R_{60\times60}\{(0,y_1),(x,20)\} = \frac{1}{30}\sum_{j=1}^{60}\frac{U_{59}^{(j)}(S_{1,j}^2+S_{2,j}^2)-2(U_{x-1}^{(j)}+U_{59-x}^{(j)})S_{1,j}S_{2,j}}{U_{60}^{(j)}-U_{58}^{(j)}-2}, \tag{49}$$

where

$$U_k^{(j)} = U_k^{(j)}(\cosh\psi_j) = \frac{\sinh(k+1)\psi_j}{\sinh\psi_j}, \quad \cosh\psi_j = \frac{\kappa_j}{2},\ k = 0,\ 1,\ \ldots,\ n, \tag{50}$$

$$\kappa_j = 4 - 2\cos\frac{(2j-1)\pi}{120}, \tag{51}$$

$$S_{1,j} = \sin\frac{y_1(2j-1)\pi}{120}, \quad S_{2,j} = \sin\frac{20(2j-1)\pi}{120}. \tag{52}$$

The 3D distribution of the equivalent resistance is shown in Fig. 7.

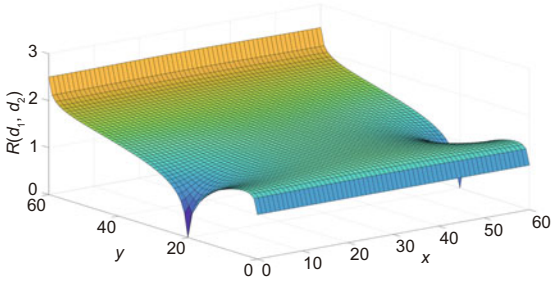

Fig. 7 The equivalent resistance view of $R_{60\times60}(d_1, d_2)$ with a cobweb resistance network shown in Eq. (49)

5 Efficiency of calculation methods

For the $(m \times n)$-scale resistance network model, $(0, y_1)$ represents the input point of the current, and (x, y_2) represents the output point of the current. We compare the efficiency of resistance calculation between two methods from point $O(0, 0)$ to any point (x, y_2).

The experiments were conducted under the following environmental conditions: CPU model Intel® Core™ i5-9300H @2.40 GHz, with MATLAB R2023a.

Remark 3 By comparing the data in Tables 1–3, we can clearly observe that the optimized equivalent resistance formula (7) exhibits a significant advantage in computational efficiency compared with the original equivalent resistance formula (1) as the network scale gradually expands under the premise that the resistance ratio remains unchanged. When the scale increases to a certain extent, the original formula is no longer suitable for numerical calculations, but is suitable for the optimized formula. In addition, we can find that the resistivity (r/r_0) has a significant effect on the calculation of the equivalent resistance while keeping the network size consistent.

Remark 4 As can be observed from Fig. 8, when the total number of nodes (i.e., $m \times n$) in the resistance network is kept constant, the time required for computation shows an increasing trend as m increases. However, regardless of these variations, the computational efficiency of Eq. (7) is always higher than that of Eq. (1). In Fig. 9, where we keep m constant, the computation time increases significantly when $n > 500$. Similarly,

Table 1 Comparison of computational efficiency for equivalent resistance formulas (1) and (7) at $h=1$*

$m\times n$	r	r_0	t_1 (s)	t_2 (s)
100×100	1	1	0.7799	0.2353
500×500	1	1	92.0133	24.0147
1000×500	1	1	380.6860	98.6743
800×800	1	1	357.9222	91.4097
1000×1000	1	1	652.8197	180.2885
1500×1000	1	1	–	404.4679

* $m\times n$ is the number of nodes in the resistance network; "–" denotes the operation time > 1200 s or beyond the memory limit of MATLAB; t_1 and t_2 refer to the CPU time in seconds consumed for resistance calculation utilizing Eqs. (1) and (7), respectively

Table 2 Comparison of computational efficiency for equivalent resistance formulas (1) and (7) at $h=10$*

$m\times n$	r	r_0	t_1 (s)	t_2 (s)
100×100	1	0.1	0.7827	0.2290
500×500	1	0.1	78.4835	21.8411
1000×500	1	0.1	316.9167	88.1708
800×800	1	0.1	300.1308	84.5293
1000×1000	1	0.1	577.8685	187.3093
1500×1000	1	0.1	–	369.5674

* $m\times n$ is the number of nodes in the resistance network; "–" denotes the operation time > 1200 s or beyond the memory limit of MATLAB; t_1 and t_2 refer to the CPU time in seconds consumed for resistance calculation utilizing Eqs. (1) and (7), respectively

Table 3 Comparison of computational efficiency for equivalent resistance formulas (1) and (7) at $h=0.1$*

$m\times n$	r	r_0	t_1 (s)	t_2 (s)
100×100	0.1	1	0.7750	0.3874
500×500	0.1	1	113.9321	25.6996
1000×500	0.1	1	385.4453	101.4138
800×800	0.1	1	400.6745	103.6280
1000×1000	0.1	1	786.0421	206.0119
1500×1000	0.1	1	–	458.0859

* $m\times n$ is the number of nodes in the resistance network; "–" denotes the operation time > 1200 s or beyond the memory limit of MATLAB; t_1 and t_2 refer to the CPU time in seconds consumed for resistance calculation utilizing Eqs. (1) and (7), respectively

Fig. 10 demonstrates the comparison of computational efficiency before and after optimization of the resistance formula when n is kept constant and m is gradually increased. The computation time increases significantly when $m > 1000$. In particular, the computation time of Eq. (1) increases more significantly. Combining the data in Figs. 8–10, it can be clearly seen that the optimized equivalent resistance formula (7) exhibits significant superiority when dealing with large-scale networks.

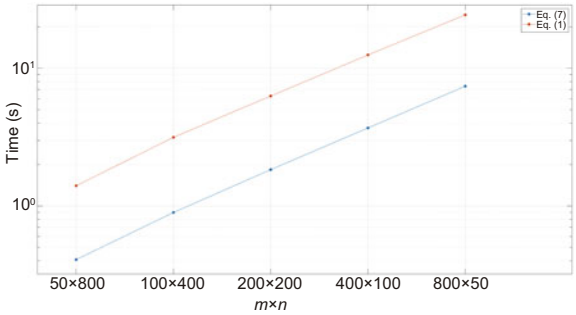

Fig. 8 Comparison of computational efficiency between Eqs. (1) and (7) when $h=1$ (the vertical axis represents the total CPU time measured in seconds)

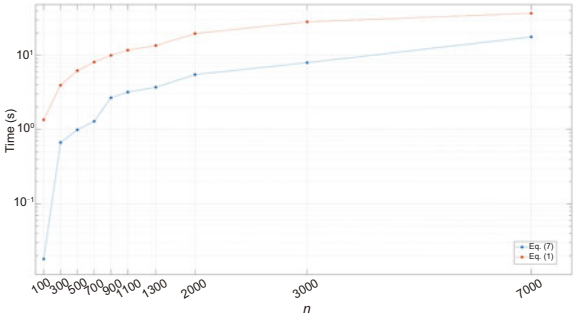

Fig. 9 Comparison of computational efficiency between Eqs. (1) and (7) as n increases, with $h=1$ and $m=100$ (the vertical axis represents the total CPU time measured in seconds)

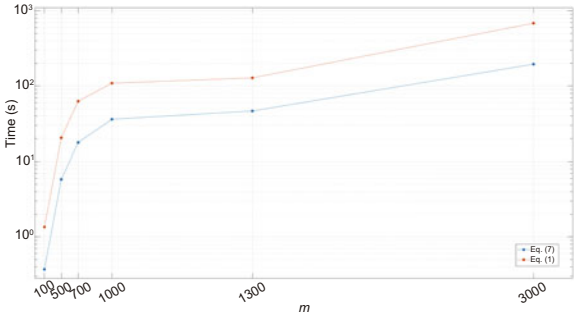

Fig. 10 Comparison of computational efficiency between Eqs. (1) and (7) as m increases, with $h=1$ and $n=100$ (the vertical axis represents the total CPU time measured in seconds)

6 An application of the potential function

Tan (2017) first used the voltage-based matrix recursive transformation (RT-V) method to study the cobweb resistance network and derived the potential function of the cobweb resistance network.

Zhao et al. (2023) optimized the potential function of the cobweb resistance network and proposed the cobweb resistance network potential function expressed by Chebyshev polynomials of the second kind. The potential function of the cobweb resistance network is as follows (Zhao et al., 2023):

$$\frac{U_{m\times n}(x,y)}{J}=\frac{4r}{2m+1}\sum_{l=1}^{m}\frac{\mu_{x_1,x}^{(l)}S_{y_1,l}-\mu_{x_2,x}^{(l)}S_{y_2,l}}{U_n^{(l)}-U_{n-2}^{(l)}-2}S_{y,l}, \tag{53}$$

where

$$\mu_{x_s,x}^{(l)}=U_{n-|x_s-x|-1}^{(l)}+U_{|x_s-x|-1}^{(l)}, s=1,\ 2, \tag{54}$$

$$S_{y_k,l}=\sin\left(\frac{y_k(2l-1)\pi}{2m+1}\right), k=1,\ 2, \tag{55}$$

$$\omega_l=2+\frac{2r}{r_0}-\frac{2r}{r_0}\cos\frac{(2l-1)\pi}{2m+1}, \tag{56}$$

$$\begin{gathered}U_v^{(l)}=U_v^{(l)}(\cosh\phi_l)=\frac{\sinh(v+1)\phi_l}{\sinh\phi_l},\\ \cosh\phi_l=\frac{\omega_l}{2},\ \frac{\omega_l}{2}>1,\ \phi_l>0,\end{gathered} \tag{57}$$

$$\begin{gathered}v=n-|x_s-x|-1,\ |x_s-x|-1,\ n-2,\ n,\\ s=1,\ 2,\ l=1,\ 2,\ldots,\ m.\end{gathered}$$

The exact potential function of cobweb is based on the research by Zhao et al. (2023). This section carefully studies and designs a path planning strategy specifically for the cobweb environment, namely the exact potential energy formula-based path planning method. The method adopts a heuristic algorithm, and its core principle is to realize effective path planning through the direction of the node with the greatest potential energy decline. In the cobweb environment, the input and output points of the current correspond to the highest and lowest potential nodes, respectively. The potential distribution is characterized by an irregular natural decline from the high-potential node to the low-potential node. In the case of obstacles, the nodes corresponding to the obstacle position are weighted by a high potential. Ultimately, a collision-free optimization path will be formed from the highest potential point to the lowest potential point. Next, we will provide a detailed introduction to the implementation details of the path planning algorithm (Algorithm 1).

Fig. 11 shows a simulation conducted in the physical environment of a 10×16 cobweb with obstacles. Let $x_1=11$, $y_1=9$, $x_2=6$, $y_2=2$, $r=1$, $r_0=1$, and $J=1$. We can derive the discrete distribution potential diagram based on the optimized Eq. (53) proposed by Zhao et al. (2023). The discrete distribution of electric potential is shown in Fig. 12.

Algorithm 1 Path planning algorithm

Step 1	Establish a map of the robot's working environment using the grid method (determine the robot's starting point, target point, and obstacles).
Step 2	The current input point in the cobweb resistance network is the starting point, and the current output point is the target point. Use Eq. (53) to calculate the potential $\frac{U(x,y)}{J}$ of each node in the cobweb resistance network.
Step 3	Add a fixed increment to the potential of the corresponding nodes that correspond to the grid points where obstacles are located in the cobweb resistance network. The potential after adding a fixed increment is $\frac{U(x,y)}{J}+0.3\frac{U(x_1,y_1)}{J}$.
Step 4	Use $\min\{U(x+1,y+1),U(x-1,y-1),U(x+1,y-1),U(x-1,y+1),U(x-1,y),U(x,y-1),U(x+1,y),U(x,y+1)\}$ to identify the node with the minimum potential.
Step 5	Move the robot to the corresponding grid point based on the node identified in Step 4 and update the current location.
Step 6	If the robot's current location matches the target point, terminate the algorithm; otherwise, proceed to Step 4.
Step 7	End of the algorithm.

In an environment with obstacles, the node potential value corresponding to the location of each obstacle was weighted. This strategy allows the robot to efficiently avoid obstacles during path planning, enabling smooth obstacle avoidance operations. This ensures that the final path is optimized to move from the high-potential node to the low-potential node. Subsequently, we demonstrate this effect through a simulation, where Fig. 13 shows the path planning in a node-weighted potential distribution map. Additionally, Fig. 14 corresponds to the robot path planning in a physical cobweb environment. Through this example, we can clearly see the application effect of the cobweb resistance network in path planning.

Looking ahead, we will comprehensively use various strategies such as gradient descent and the

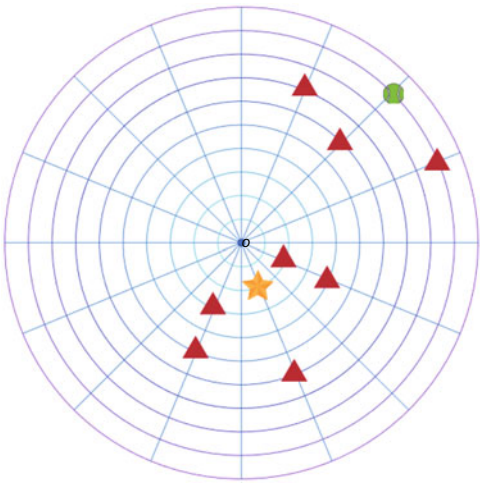

Fig. 11 A physical map of a 10×16 cobweb with obstacles. The red triangles represent the obstacles, the green ball represents the starting point, and the yellow five-pointed star represents the end point. References to color refer to the online version of this figure

establishment of subgoals to further delve into robot path planning in cobweb environments with obstacles, aiming to achieve more precise and efficient planning results.

7 Conclusions

In this paper, the equivalent resistance formula between two points of an $m \times n$ cobweb resistance network with a $2r$ boundary has been improved using Chebyshev polynomials of the second kind combined with hyperbolic functions. The optimized equivalent resistance formula (7) cleverly utilizes the optimal approximation property of Chebyshev polynomials, which not only improves the computational efficiency but also simplifies the derivation process. Based on the comparison of the computational efficiency of the equivalent resistance formula before and after optimization, it is found that the computational efficiency is improved by more than three times at the same scale. This is especially obvious as the size of the resistance network increases. In addition, considering the influence of parameters on the equivalent resistance formula, we discussed the equivalent resistance formula for several special cases, which have been presented through 3D dynamic views.

Additionally, we attempted to perform path planning with respect to the cobweb potential function and successfully developed a heuristic algorithm to accomplish path planning by simulating potential descent. The process of finding paths in this algorithm is actually an exploration using the numerical results of the potentials to find the paths on the circuit from the input point to the output point. In an environment with obstacles, weighting the value of the node potential at the obstacle enables the robot to effectively avoid the obstacle during the path planning process and ensures that the robot can

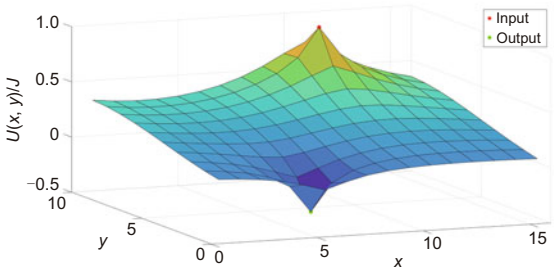

Fig. 12 Obstacle-free potential distribution diagram

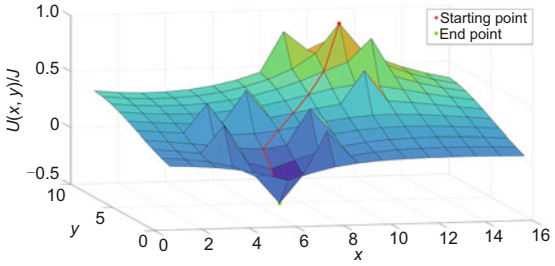

Fig. 13 Path planning in a node-weighted potential distribution map

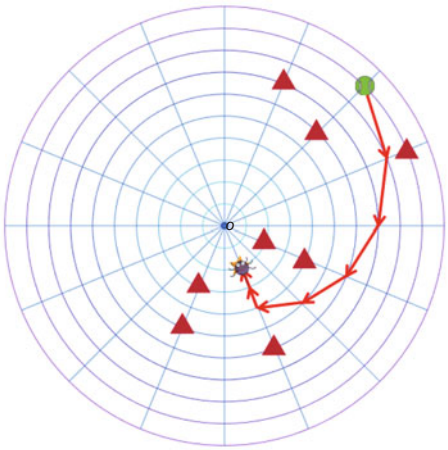

Fig. 14 Robot path planning in a physical cobweb environment. The green ball represents the starting point, the yellow five-pointed star represents the end point, and the red triangles represent the obstacles. The purple spider represents the robot, and the solid lines with red arrows represent the robot's path. References to color refer to the online version of this figure

quickly approach the target point from the starting point based on the potential descent trend. The effectiveness of the algorithm has also been demonstrated through specific numerical simulations.

Contributors

Xiaoyu JIANG and Yanpeng ZHENG conceived the project and performed formula calculations. Zhaolin JIANG proposed an improved formula for calculating equivalent resistance. Yu GUAN validated the correctness of formula calculation, drew the graphs, and drafted, revised, and finalized this paper.

Conflict of interest

All the authors declare that they have no conflict of interest.

Data availability

The data that support the findings of this study are available from the corresponding authors upon reasonable request.

References

Asad JH, 2013a. Exact evaluation of the resistance in an infinite face-centered cubic network. *J Stat Phys*, 150(6):1177-1182. https://doi.org/10.1007/s10955-013-0716-x

Asad JH, 2013b. Infinite simple 3D cubic network of identical capacitors. *Mod Phys Lett B*, 27(15):1350112. https://doi.org/10.1142/S0217984913501121

Asad JH, Diab AA, Hijjawi RS, et al., 2013. Infinite face-centered-cubic network of identical resistors: application to lattice Green's function. *Eur Phys J Plus*, 128(1):2. https://doi.org/10.1140/epjp/i2013-13002-8

Chen JQ, Ji WY, Tan ZZ, 2024. Electrical properties of a $2 \times n$ non-regular hammock network. *Indian J Phys*, 98(8):2851-2860. https://doi.org/10.1007/s12648-023-03027-w

Cserti J, Dávid G, Piróth A, 2002. Perturbation of infinite networks of resistors. *Am J Phys*, 70(2):153-159. https://doi.org/10.1119/1.1419104

Cserti J, Széchenyi G, Dávid G, 2011. Uniform tiling with electrical resistors. *J Phys A Math Theor*, 44(21):215201. https://doi.org/10.1088/1751-8113/44/21/215201

Essam JW, Wu FY, 2009. The exact evaluation of the corner-to-corner resistance of an $M \times N$ resistor network: asymptotic expansion. *J Phys A Math Theor*, 42(2):025205. https://doi.org/10.1088/1751-8113/42/2/025205

Essam JW, Tan ZZ, Wu FY, 2014. Resistance between two nodes in general position on an $m \times n$ fan network. *Phys Rev E*, 90(3):032130. https://doi.org/10.1103/PhysRevE.90.032130

Essam JW, Izmailyan NS, Kenna R, et al., 2015. Comparison of methods to determine point-to-point resistance in nearly rectangular networks with application to a 'hammock' network. *R Soc Open Sci*, 2(4):140420. https://doi.org/10.1098/rsos.140420

Ferri G, Antonini G, 2007. Ladder-network-based model for interconnects and transmission lines time delay and cutoff frequency determination. *J Circ Syst Comp*, 16(4):489-505. https://doi.org/10.1142/S0218126607003794

Fu YR, Jiang XY, Jiang ZL, et al., 2020a. Inverses and eigenpairs of tridiagonal Toeplitz matrix with opposite-bordered rows. *J Appl Anal Comput*, 10(4):1599-1613. https://doi.org/10.11948/20190287

Fu YR, Jiang XY, Jiang ZL, et al., 2020b. Properties of a class of perturbed Toeplitz periodic tridiagonal matrices. *Comput Appl Math*, 39(3):146. https://doi.org/10.1007/s40314-020-01171-1

Giordano S, 2007. Two-dimensional disordered lattice networks with substrate. *Phys A*, 375(2):726-740. https://doi.org/10.1016/j.physa.2006.09.026

Guttmann AJ, 2010. Lattice Green's functions in all dimensions. *J Phys A Math Theor*, 43(30):305205. https://doi.org/10.1088/1751-8113/43/30/305205

Hadad Y, Soric JC, Khanikaev AB, et al., 2018. Self-induced topological protection in nonlinear circuit arrays. *Nat Electron*, 1(3):178-182. https://doi.org/10.1038/s41928-018-0042-z

Hijjawi RS, Asad JH, Sakaji AJ, et al., 2008. Infinite simple 3D cubic lattice of identical resistors (two missing bonds). *Eur Phys J Appl Phys*, 41(2):111-114. https://doi.org/10.1051/epjap:2008015

Hu Q, Zheng B, 2023. An efficient Takagi–Sugeno fuzzy zeroing neural network for solving time-varying Sylvester equation. *IEEE Trans Fuzzy Syst*, 31(7):2401-2411. https://doi.org/10.1109/TFUZZ.2022.3225630

Izmailian NS, Huang MC, 2010. Asymptotic expansion for the resistance between two maximally separated nodes on an M by N resistor network. *Phys Rev E*, 82(1):011125. https://doi.org/10.1103/PhysRevE.82.011125

Izmailian NS, Kenna R, 2014. A generalised formulation of the Laplacian approach to resistor networks. *J Stat Mech Theory Exp*, 9:P09016. https://doi.org/10.1088/1742-5468/2014/09/P09016

Izmailian NS, Kenna R, 2015. The two-point resistance of fan networks. *Chin J Phys*, 53(1):126-136. https://doi.org/10.6122/CJP.20141020A

Izmailian NS, Kenna R, Wu FY, 2014. The two-point resistance of a resistor network: a new formulation and application to the cobweb network. *J Phys A Math Theor*, 47(3):035003. https://doi.org/10.1088/1751-8113/47/3/035003

Ji YX, Ni LT, Zhao C, et al., 2023. Tripfield: a 3D potential field model and its applications to local path planning of autonomous vehicles. *IEEE Trans Intell Transp Syst*, 24(3):3541-3554. https://doi.org/10.1109/TITS.2022.3231259

Jiang XY, Zhang GJ, Zheng YP, et al., 2024. Explicit potential function and fast algorithm for computing potentials in $\alpha \times \beta$ conic surface resistor network. *Expert Syst Appl*, 238:122157. https://doi.org/10.1016/j.eswa.2023.122157

Jiang ZL, Wang WP, Zheng YP, et al., 2019. Interesting explicit expressions of determinants and inverse matrices for Foeplitz and Loeplitz matrices. *Mathematics*, 7(10):939. https://doi.org/10.3390/math7100939

Jiang ZL, Zhou YF, Jiang XY, et al., 2023. Analytical potential formulae and fast algorithm for a horn torus resistor network. *Phys Rev E*, 107(4):044123. https://doi.org/10.1103/PhysRevE.107.044123

Jin L, Qi YM, Luo X, et al., 2022a. Distributed competition of multi-robot coordination under variable and switching topologies. *IEEE Trans Autom Sci Eng*, 19(4):3575-3586. https://doi.org/10.1109/TASE.2021.3126385

Jin L, Zheng X, Luo X, 2022b. Neural dynamics for distributed collaborative control of manipulators with time delays. *IEEE/CAA J Autom Sin*, 9(5):854-863. https://doi.org/10.1109/JAS.2022.105446

Kirchhoff G, 1847. Ueber die auflösung der gleichungen, auf welche man bei der untersuchung der linearen vertheilung galvanischer ströme geführt wird. *Ann Phys*, 148(12):497-508 (in German). https://doi.org/10.1002/andp.18471481202

Klein DJ, 2010. Centrality measure in graphs. *J Math Chem*, 47(4):1209-1223. https://doi.org/10.1007/s10910-009-9635-0

Klein DJ, Randić M, 1993. Resistance distance. *J Math Chem*, 12(1):81-95. https://doi.org/10.1007/BF01164627

Kook W, 2011. Combinatorial Green's function of a graph and applications to networks. *Adv Appl Math*, 46(1-4):417-423. https://doi.org/10.1016/j.aam.2010.10.006

Kulathunga G, 2022. A reinforcement learning based path planning approach in 3D environment. *Proc Comput Sci*, 212:152-160. https://doi.org/10.1016/j.procs.2022.10.217

Liu YJ, Meirer F, Krest CM, et al., 2016. Relating structure and composition with accessibility of a single catalyst particle using correlative 3-dimensional microspectroscopy. *Nat Commun*, 7(1):12634. https://doi.org/10.1038/ncomms12634

Luo XL, Tan ZZ, 2023. Fractional circuit network theory with n-V-structure. *Phys Scr*, 98(4):045224. https://doi.org/10.1088/1402-4896/acc491

Mahulea C, Kloetzer M, González R, 2020. Path Planning of Cooperative Mobile Robots Using Discrete Event Models. Wiley-IEEE Press, Piscataway, USA. https://doi.org/10.1002/9781119486305

Mason JC, Handscomb DC, 2002. Chebyshev Polynomials. Chapman and Hall/CRC, New York, USA, p.360. https://doi.org/10.1201/9781420036114

Mazaheri H, Goli S, Nourollah A, 2024. Path planning in three-dimensional space based on butterfly optimization algorithm. *Sci Rep*, 14(1):2332. https://doi.org/10.1038/s41598-024-52750-9

Meng QY, Jiang XY, Jiang ZL, 2021. Interesting determinants and inverses of skew Loeplitz and Foeplitz matrices. *J Appl Anal Comput*, 11(6):2947-2958. https://doi.org/10.11948/20210070

Meng QY, Zheng YP, Jiang ZL, 2022a. Determinants and inverses of weighted Loeplitz and weighted Foeplitz matrices and their applications in data encryption. *J Appl Math Comput*, 68(6):3999-4015.

Meng QY, Zheng YP, Jiang ZL, 2022b. Exact determinants and inverses of (2,3,3)-Loeplitz and (2,3,3)-Foeplitz matrices. *Comp Appl math*, 41(1):35. https://doi.org/10.1007/s40314-021-01738-6

Meng X, Jiang XY, Zheng YP, et al., 2024. A novel formula for representing the equivalent resistance of the $m \times n$ cylindrical resistor network. *Sci Rep*, 14:21254. https://doi.org/10.1038/s41598-024-72196-3

Owaidat MQ, Hijjawi RS, Khalifeh JM, 2012. Network with two extra interstitial resistors. *Int J Theor Phys*, 51(10):3152-3159. https://doi.org/10.1007/s10773-012-1196-5

Pan ZH, Zhang CX, Xia YQ, et al., 2022. An improved artificial potential field method for path planning and formation control of the multi-UAV systems. *IEEE Trans Circ Syst II Express Briefs*, 69(3):1129-1133. https://doi.org/10.1109/TCSII.2021.3112787

Pennetta C, Alfinito E, Reggiani L, et al., 2004. Biased resistor network model for electromigration failure and related phenomena in metallic lines. *Phys Rev B*, 70(17):174305. https://doi.org/10.1103/PhysRevB.70.174305

Rhazaoui K, Cai Q, Adjiman CS, et al., 2013. Towards the 3D modeling of the effective conductivity of solid oxide fuel cell electrodes: I. model development. *Chem Eng Sci*, 99:161-170. https://doi.org/10.1016/j.ces.2013.05.030

Shi Y, Jin L, Li S, et al., 2022. Novel discrete-time recurrent neural networks handling discrete-form time-variant multi-augmented Sylvester matrix problems and manipulator application. *IEEE Trans Neur Netw Learn Syst*, 33(2):587-599. https://doi.org/10.1109/TNNLS.2020.3028136

Sun ZB, Wang G, Jin L, et al., 2022. Noise-suppressing zeroing neural network for online solving time-varying matrix square roots problems: a control-theoretic approach. *Expert Syst Appl*, 192:116272. https://doi.org/10.1016/j.eswa.2021.116272

Tan ZZ, 2017. Recursion-transform method and potential formulae of the $m \times n$ cobweb and fan networks. *Chin Phys B*, 26(9):090503. https://doi.org/10.1088/1674-1056/26/9/090503

Tan ZZ, 2022. Resistance theory for two classes of n-periodic networks. *Eur Phys J Plus*, 137(5):546. https://doi.org/10.1140/epjp/s13360-022-02750-3

Tan ZZ, 2023a. Electrical property of an $m \times n$ apple surface network. *Results Phys*, 47:106361. https://doi.org/10.1016/j.rinp.2023.106361

Tan ZZ, 2023b. Theory of an $m \times n$ apple surface network with special boundary. *Commun Theor Phys*, 75(6):065701. https://doi.org/10.1088/1572-9494/accb82

Tan ZZ, Fang JH, 2015. Two-point resistance of a cobweb network with a $2r$ boundary. *Commun Theor Phys*, 63(1):36. https://doi.org/10.1088/0253-6102/63/1/07

Tan ZZ, Tan Z, 2020a. The basic principle of $m \times n$ resistor networks. *Commun Theor Phys*, 72(5):055001. https://doi.org/10.1088/1572-9494/ab7702

Tan ZZ, Tan Z, 2020b. Electrical properties of $m \times n$ cylindrical network. *Chin Phys B*, 29(8):080503. https://doi.org/10.1088/1674-1056/ab96a7

Tan ZZ, Tan Z, 2020c. Electrical properties of an $m \times n$ rectangular network. *Phys Scr*, 95(3):035226. https://doi.org/10.1088/1402-4896/ab5977

Tan ZZ, Zhou L, Yang JH, 2013. The equivalent resistance of a $3 \times n$ cobweb network and its conjecture of an $m \times n$ cobweb network. *J Phys A Math Theor*, 46(19):195202. https://doi.org/10.1088/1751-8113/46/19/195202

Tzeng WJ, Wu FY, 2006. Theory of impedance networks: the two-point impedance and *LC* resonances. *J Phys A Math Gen*, 39(27):8579. https://doi.org/10.1088/0305-4470/39/27/002

Udrea G, 1996. A note on the sequence $(w_n)_{n\geq 0}$ of A.F. Horadam. *Port Math*, 53(2):143-155.

Uğur A, 2008. Path planning on a cuboid using genetic algorithms. *Inform Sci*, 178(16):3275-3287. https://doi.org/10.1016/j.ins.2008.04.005

Wang JJ, Zheng YP, Jiang ZL, 2023. Norm equalities and inequalities for tridiagonal perturbed Toeplitz operator matrices. *J Appl Anal Comput*, 13(2):671-683. https://doi.org/10.11948/20210489

Wang R, Jiang XY, Zheng YP, et al., 2024. New equivalent resistance formula of $m \times n$ rectangular resistor network represented by Chebyshev polynomials. *Sci Rep*, 14:29461. https://doi.org/10.1038/s41598-024-80899-w

Wang XZ, Che ML, Wei YM, 2017. Complex-valued neural networks for the Takagi vector of complex symmetric matrices. *Neurocomputing*, 223:77-85. https://doi.org/10.1016/j.neucom.2016.10.034

Wei YL, Jiang XY, Jiang ZL, et al., 2019a. Determinants and inverses of perturbed periodic tridiagonal Toeplitz matrices. *Adv Differ Equ*, 2019(1):410. https://doi.org/10.1186/s13662-019-2335-6

Wei YL, Zheng YP, Jiang ZL, et al., 2019b. A study of determinants and inverses for periodic tridiagonal Toeplitz matrices with perturbed corners involving Mersenne numbers. *Mathematics*, 7(10):893. https://doi.org/10.3390/math7100893

Wei YL, Jiang XY, Jiang ZL, et al., 2020. On inverses and eigenpairs of periodic tridiagonal Toeplitz matrices with perturbed corners. *J Appl Anal Comput*, 10(1):178-191. https://doi.org/10.11948/20190105

Wei YL, Zheng YP, Jiang ZL, et al., 2022. The inverses and eigenpairs of tridiagonal Toeplitz matrices with perturbed rows. *J Appl Math Comput*, 68(1):623-636. https://doi.org/10.1007/s12190-021-01532-x

Wu FY, 2004. Theory of resistor networks: the two-point resistance. *J Phys A Math Gen*, 37(26):6653-6673. https://doi.org/10.1088/0305-4470/37/26/004

Wu WQ, Zhang YN, 2024. Zeroing neural network with coefficient functions and adjustable parameters for solving time-variant Sylvester equation. *IEEE Trans Neur Netw Learn Syst*, 35(5):6757-6766. https://doi.org/10.1109/TNNLS.2022.3212869

Xu GY, Eleftheriades GV, Hum SV, 2021. Analysis and design of general printed circuit board metagratings with an equivalent circuit model approach. *IEEE Trans Antenn Propagat*, 69(8):4657-4669. https://doi.org/10.1109/TAP.2021.3060084

Xue JM, Li J, Chen JY, et al., 2021. Wall-climbing robot path planning for cylindrical storage tank inspection based on modified A-star algorithm. IEEE Far East NDT New Technology & Application Forum, p.191-195. https://doi.org/10.1109/FENDT54151.2021.9749634

Yang YJ, Klein DJ, 2013. A recursion formula for resistance distances and its applications. *Discret Appl Math*, 161(16-17):2702-2715. https://doi.org/10.1016/j.dam.2012.07.015

Yu ZH, Yuan J, Li YS, et al., 2023. A path planning algorithm for mobile robot based on water flow potential field method and beetle antennae search algorithm. *Comput Electr Eng*, 109:108730. https://doi.org/10.1016/j.compeleceng.2023.108730

Zhang D, Yang B, Tan JP, et al., 2021. Impact damage localization and mode identification of CFRPs panels using an electric resistance change method. *Compos Struct*, 276:114587. https://doi.org/10.1016/j.compstruct.2021.114587

Zhao WJ, Zheng YP, Jiang XY, et al., 2023. Two optimized novel potential formulas and numerical algorithms for $m \times n$ cobweb and fan resistor networks. *Sci Rep*, 13(1):12417. https://doi.org/10.1038/s41598-023-39478-8

Zhou YF, Zheng YP, Jiang XY, et al., 2022. Fast algorithm and new potential formula represented by Chebyshev polynomials for an $m \times n$ globe network. *Sci Rep*, 12(1):21260. https://doi.org/10.1038/s41598-022-25724-y

Zhou YF, Jiang XY, Zheng YP, et al., 2023. Exact novel formulas and fast algorithm of potential for a hammock resistor network. *AIP Adv*, 13(9):095127. https://doi.org/10.1063/5.0171330

Zhu ZX, Yin Y, Lü HG, 2023. Automatic collision avoidance algorithm based on route-plan-guided artificial potential field method. *Ocean Eng*, 271:113737. https://doi.org/10.1016/j.oceaneng.2023.113737